VIP Anion–π Catalysis Very Important Paper

International Edition: DOI: 10.1002/anie.201804092
German Edition: DOI: 10.1002/ange.201804092

Remote Control of Anion–π Catalysis on Fullerene-Centered Catalytic Triads

Javier López-Andarias, Antonio Bauzá, Naomi Sakai, Antonio Frontera, and Stefan Matile**

Abstract: *The design, synthesis and evaluation of catalytic triads composed of a central C_{60} fullerene with an amine base on one side and polarizability enhancers on the other side are reported. According to an enolate addition benchmark reaction, fullerene–fullerene–amine triads display the highest selectivity in anion–π catalysis observed so far, whereas NDI–fullerene–amine triads are not much better than fullerene–amine controls (NDI = naphthalenediimide). These large differences in activity are in conflict with the small differences in intrinsic π acidity, that is, LUMO energy levels and π holes on the central fullerene. However, they are in agreement with the high polarizability of fullerene–fullerene–amine triads. Activation and deactivation of the fullerene-centered triads by intercalators and computational data on anion binding further indicate that for functional relevance, intrinsic π acidity is less important than induced π acidity, that is, the size of the oriented macrodipole of polarizable π systems that emerges only in response to the interaction with anions and anionic transition states. The resulting transformation is thus self-induced, the anionic intermediates and transition states create their own anion–π catalyst.*

Anion–π interactions[1] refer to the attraction between anions and aromatic surfaces. This is opposite to the conventional cation–π interaction[2] between a positive charge and a π-basic aromatic surface, and much less recognized because it is counterintuitive. Their comparable relevance is generally recognized only if the interactions are too strong and continue into either nucleophilic and electrophilic aromatic substitutions or the generation of radical anions and cations, respectively. Whereas the exact nature of anion–π interactions is still under debate, intrinsic π acidity, that is, low-lying LUMO energies, π holes (areas with positive molecular electrostatic potential (MEP), Figures 1 a,b), positive quadrupole moments perpendicular to the aromatic plane or in-plane dipoles from electron-withdrawing substituents, have received much attention, resulting in much interest in small, compact π surfaces such as, for instance, in hexafluorobenzene or naphthalenediimides (NDIs).[1,3–5] Despite much encouragement from pioneering theoretical studies,[6] induced anion–π interactions have been largely ignored in practice. However, very recent results from anion–π catalysis, that is, the stabilization of anionic transition states on aromatic surfaces,[3] revealed that activities increase in response to electric fields,[4] with increasing length of π-stacked foldamers,[5] and on fullerenes.[7] The discovery of anion–π catalysis on fullerenes was of particular interest because this most popular carbon allotrope[8] has received little attention with regard to both anion–π interactions[9] and catalysis.[10] This emerging power of polarizability[11] for anion–π catalysis called for expanded π surfaces beyond fullerenes to access induced macrodipoles as large as possible in response to anion binding (Figure 1 c). As a first step in this direction, we here report the design, synthesis and evaluation of catalytic triads composed of a central fullerene with an active site on one side and a polarizability enhancer on the other side.

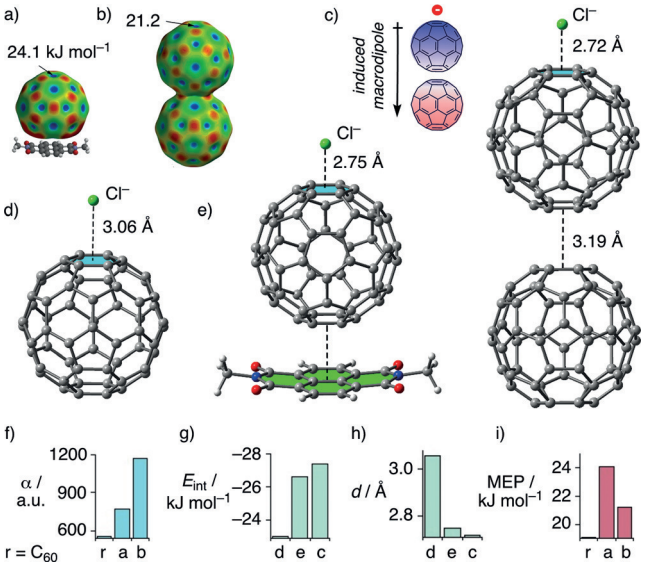

Figure 1. MEP surface of a) C_{60} stacked to Me_2NDI and b) a C_{60} dimer, optimized geometries of chloride complexes with c) $C_{60}\cdots C_{60}$ (with cartoon illustrating the anion-induced macrodipole), d) C_{60} and e) NDI$\cdots C_{60}$, and comparative summary of f) polarizability α, g) interaction energies E_{int} with Cl^-, h) Cl^-–π distances and i) deepest π holes on MEP surfaces.

[*] Dr. J. López-Andarias, Dr. N. Sakai, Prof. S. Matile
Department of Organic Chemistry, University of Geneva
Geneva (Switzerland)
E-mail: stefan.matile@unige.ch
Homepage: http://www.unige.ch/sciences/chiorg/matile/
A. Bauzá, Prof. A. Frontera
Department de Química, Universitat de les Illes Balears
Palma de Mallorca, Baleares (Spain)
E-mail: toni.frontera@uib.es
Supporting information and the ORCID identification number(s) for the author(s) of this article can be found under: https://doi.org/10.1002/anie.201804092.

Electronic communication in the ground state in fullerene–fullerene,[12] fullerene–NDI[13] and many other dyads[14] has been explored extensively. In our theoretical calculations on the BP86-D3/def2-TZVP level with dispersion correction in THF continuum, we found that the deepest π hole on the molecular electrostatic potential (MEP) surface increases by at most only 4.4 kJ mol^{-1} in the presence of an NDI or a fullerene π stacked to the other side of a fullerene (Figures 1 a,b,i). However, the polarizability of fullerene–fullerene but not NDI–fullerene dyads more than doubled compared to C_{60} (Figure 1 f). In chloride complexes, fullerene–fullerene dyads gave the largest binding energies and shortest anion···fullerene distances, thus indicating that induced π acidity is more important than intrinsic π acidity (Figures 1 c–i).

In the catalytic triad **1**, a fullerene–fullerene dyad is combined with a tertiary amine base (Scheme 1). The positioning of this base is important to turn on anion–π interactions as soon as the negative charge is injected into a substrate by proton transfer.[7] Theoretical models demonstrated that a shape-persistent cyclohexyldiamine bridge would also be suitable to bring the two fullerenes into close contact ($d = 3.09$ Å, vide infra). The fullerene–fullerene–amine triad **1** was complemented by NDI–fullerene–amine triads **2–5** with NDIs of different π acidity,[15] and fullerene–amine dyad **6** as a negative control (Scheme 1, Figures S1–S3).

The synthesis of all six anion–π catalysts started with a Bingel reaction of fullerene **7** with malonamide **8**, which was readily accessible from commercially available starting materials (Scheme 1, Schemes S1–S5). Removal of the *tert*-butyl protecting group afforded acid **9**. From this key intermediate, control **6** was obtained by coupling with amine **10**. For triad **1**, malonamide **11** with an adamantyl solubilizer was prepared first. Bingel reaction with fullerene **7**, followed by *tert*-butyl deprotection, coupling with **10** and further Boc removal afforded amine **12**, which was transformed into the target molecule by coupling with acid **9**. The series of NDIs **13–16** was prepared following previously reported procedures.[3,4] In separate reactions, the four NDIs were then first deprotected, and the obtained amines were reacted with acid **9** to afford triads **2–5**.

The UV/Vis absorption spectra of **2–5** were characterized by a hypochromic effect in the NDI region around 380 nm (Figure 2 a, Figure S5). The circular dichroism (CD) spectra

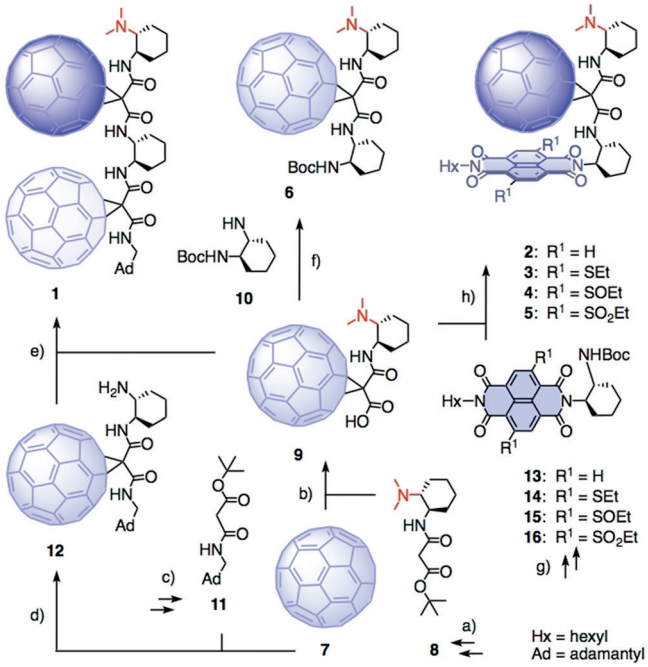

Scheme 1. a) 3-*tert*-Butoxy-3-oxopropanoic acid, (*R*,*R*)-*N*,*N*-dimethylcyclohexane-1,2-diamine, HBTU, TEA, CH_2Cl_2, 20 min, RT, 87%; b) 1. I_2, DBU, toluene, 2 h, RT, 57%; 2. TFA, CH_2Cl_2, RT, overnight, quant.; c) 3-*tert*-butoxy-3-oxopropanoic acid, 1-adamantanemethylamine, HBTU, TEA, CH_2Cl_2, 1 h, RT, 95%; d) 1. I_2, DBU, toluene, 2 h, RT, 41%; 2. TFA, CH_2Cl_2, RT, overnight, 97%; 3. **10**, HBTU, TEA, CH_2Cl_2, 3 h, RT, 88%; 4. TFA, CH_2Cl_2, RT, 2 h, quant.; e) HBTU, TEA, CH_2Cl_2, RT, overnight, 55%; f) HBTU, TEA, CH_2Cl_2, 4 h, RT, 90%; g) see the Supporting Information; h) 1. TFA, CH_2Cl_2, RT, 2 h, quant.; 2. HBTU, TEA, CH_2Cl_2, RT, 4 h, 73% (**2**), 57% (**3**), 56% (**4**), 49% (**5**). HBTU = 2-(1*H*-benzotriazol-1-yl)-1,1,3,3-tetramethyluronium hexafluorophosphate, DBU = 1,8-diazabicyclo[5.4.0]undec-7-ene, TFA = trifluoroacetic acid.

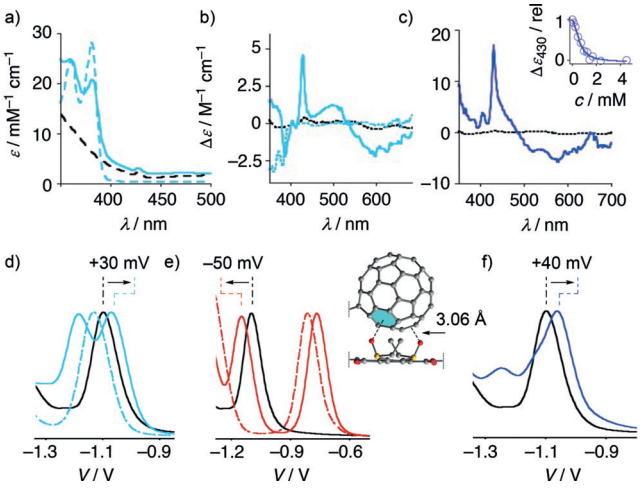

Figure 2. a) UV/Vis absorption spectra of **2** (cyan), **6** (black) and **13** (dotted cyan) in $CHCl_3$. b) CD spectra of **2** (cyan), **6** (black) and **13** (dotted cyan) in $CHCl_3$. c) CD spectra of **1** (purple), **6** (black); inset: CD of **1** at 430 nm with increasing concentrations of **21**. d) DPV of **2** (cyan), **6** (black) and **13** (dotted cyan). e) DPV of **4** (red), **6** (black), **15** (dotted red), with pertinent part of the energy-minimized structure of **4**. f) DPV of **1** (purple) and **6** (black). DPV was performed in CH_2Cl_2 with tetrabutylammonium hexafluorophosphate ($TBAPF_6$, 0.1 M) as the supporting electrolyte and Fc^+/Fc as the internal reference.

of **1–5** contained strong positive and negative CD Cotton effects from 350 nm up to 700 nm (Figure 2 b,c, Figure S6). The π-stacked immobilization of the NDIs and the second fullerene in the (+)-sector[16] of the central fullerene conceivably accounted for the distinct positive CD Cotton effect at 430 nm, whereas Boc and amine termini were insufficiently immobilized on the fullerene surface to afford a strong induced CD for **6**. All these spectroscopic characteristics supported strong electronic coupling between the two chromophores in the respective dyads.

The redox properties were determined by cyclic (CV) and differential pulse voltammetry (DPV) versus Fc^+/Fc as

Table 1: Characteristics of catalysts.

Entry	Cat.[a]	ΔV [mV][b]	MEP [kJ mol^{-1}][c]	α [a.u.][d]	A/D$_1$[e]	A/D$_2$[f]
1	TEA	–	–	–	0.6	1.8
2	**6**	0	13.8	903	2.3	8.2
3	**2**	+30	16.6	1016	2.7	9.2
4	**3**	0	14.2	1130	1.6	6.1
5	**4**	−50	15.7	1141	2.2	7.6
6	**5**	−140	17.0	1127	2.0	6.3
7	**1**	+40	13.9	1499	5.2	22.5

[a] Catalysts, see Scheme 1; TEA = triethylamine. [b] Difference between the first reduction potential of fullerene within the catalysts and the first reduction potential of control **6** (from DPV experiments). [c] Highest positive potential on the MEP surfaces of the central fullerenes. [d] Computed polarizability. [e] Yield of addition/yield of decarboxylation. Reactions were conducted with 20 mol% catalyst **1**–**6**, 200 mM **17** and 2.0 M **18** and at 20°C in [D$_8$]THF, and monitored by ^{1}H NMR spectroscopy. [f] As with [e] in [D$_8$]THF/CDCl$_3$ 1:1.

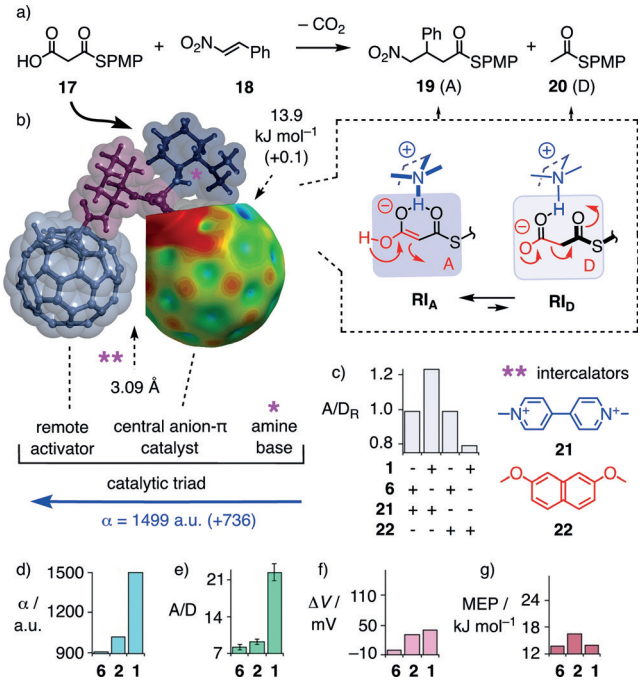

Figure 3. a) The base-catalyzed reaction between MAHT **17** (PMP: *p*-methoxyphenyl) and enolate acceptor **18** to afford addition product **19** (A) or decarboxylation product **20** (D). b) Energy-minimized cutaway structure of triad **1** (without adamantyl solubilizer), with indication of the equilibrium control between reactive intermediates **RI$_A$** and **RI$_D$** on the central fullerene by the remote fullerene and intercalators **21** (PF_6^- salt) and **22**. c) A/D$_R$ values of catalysts **1** and **6** (40 mM) in the absence and presence of **21** or **22** (800 mM; 200 mM **17**, 2 M **18**, [D$_8$]THF/CDCl$_3$ 1:1; A/D$_R$ = A/D$_{(1+21)}$/ A/D$_{(1)}$, etc). d–g) Comparative summary of d) polarizability α, e) catalysis (A/D values), f) first fullerene reduction potential relative to **6** and g) deepest π holes on MEP surfaces for catalysts **1**, **2** and **6** (compare Table 1).

internal standard. The first irreversible reduction potential of **1** appeared + 40 mV compared to **6** (Figure 2 f, Figures S7 and S8, Table 1). Results from fullerene dimers in the literature[12] confirmed that electron sharing accounts for this lowering of the LUMO energy.

In NDI–fullerene **2**, lowered and raised LUMO levels for fullerenes (irreversible, + 30 mV) and NDIs (reversible, −50 mV), respectively, were consistent with the increasing intrinsic π acidity of the fullerene due to the transfer of electron density to the NDI (Figure 2 d, Figures S7 and S8, Table 1). In **3**, the NDI has two sulfide donors in the core. Consistent with the weaker π acidity of this NDI,[15] the LUMO level of the fullerene in **3** did not decrease (Figures S7 and S8). Conversion of the sulfide donors in **3** to sulfoxide and sulfone acceptors in the NDIs in **4** and **5** shifted the first fullerene reduction potential by −50 mV and −140 mV, respectively (Figure 2 e, Figures S7 and S8). These shifts were possibly caused by repulsive NDI radical anions. Positive shifts of the NDI reduction potentials suggested that electron density is transferred from the NDI through back-donating lonepair–π interactions from the S−O donors to the fullerene acceptors (Figure 2 e, Figure S4).

The addition of malonic acid half thioester (MAHT) **17** to nitroolefin **18** was selected to probe anion–π catalysis with triads **1**–**5** (Figure 3 a).[3–5] This transformation has emerged as the benchmark reaction. Recent computational studies have confirmed that selective recognition of the planar, charge-delocalized "enol" tautomer in reactive intermediate **RI$_A$** on π-acidic surfaces promotes the formation of the biologically relevant but disfavored addition product **19** (A), while weaker anion–π interactions with the bent, charge-localized "keto" intermediate hinder decarboxylation before enolate addition and thus the formation of the irrelevant product **20** (D, Figure 3 a,b).[5,7]

The fullerene–amine dyad **6** conceived here as a starting point was identified as a powerful anion–π catalyst that inverts the preference for decarboxylation with triethylamine (TEA) in [D$_8$]THF (A/D$_1$ = 0.6) to a preference for enolate addition (A/D$_1$ = 2.3, Table 1, entries 1 and 2; A/D: Yield of **19** divided by yield of **20**). For the catalytic NDI–fullerene–amine triad **2**, this selectivity increased to A/D$_1$ = 2.7 in [D$_8$]THF and from A/D$_2$ = 8.2 for **6** to A/D$_2$ = 9.2 for **2** in the more hydrophobic [D$_8$]THF/CDCl$_3$ 1:1 (entries 2 and 3). These results were in agreement with contributions from the remote NDI to increase the intrinsic (lower LUMO levels; + 30 mV, deeper π holes; + 2.8 kJ mol^{-1}) and the induced π acidity (higher polarizability; + 113.4 a.u.) on the active fullerene surface. As expected for the sulfide donors in the NDI core, anion–π catalysis by **3** dropped to A/D$_1$ = 1.6 and A/D$_2$ = 5.6 (entry 4). Partial recovery of activity by triad **4** suggested that higher fullerene LUMO levels (−50 mV) are compensated by higher polarizability (+ 238 a.u., entry 5). The poorer activity of triad **5** was consistent with stronger back-donating lonepair–π interactions from sulfone oxygens in the NDI core (−140 mV, entry 6).

With fullerene-fullerene-amine triad **1**, anion–π catalysis increased to A/D$_1$ = 5.2 and A/D$_2$ = 22.5 (entry 7). This activity is outstanding not only in the context of this work, it is a new record for anion–π interactions in organocatalysis (excluding anion–π enzymes).[3–5,7] The activity found for triad **1** exceeded expectations from the lowering LUMO levels of fullerenes from **6** to **2** and **1** clearly (Figures 3 e,f) and disagreed with predictions based on π holes on the central fullerene (Figures 3 e,g). However, the exceptional activity of

fullerene–fullerene–amine triad **1** corresponded well with the exceptional polarizability of triad **1** (Figures 3d,e; triads **3**–**5** could not be compared because the NDI core substituents complicate the situation, vide supra). This correlation of activity with polarizability was consistent with the functional relevance of the oriented macrodipoles that are formed only on contact with anions and anionic transition states, i.e., induced π acidity (Figure 1c).

In the presence of methyl viologen **21** (MV^{2+}),[17] the catalytic activity of triad **1** but not control **6** further increased by $A/D_{(1+21)}/A/D_{(1)} = 1.23$ (Figure 3c). CD titrations indicated that the π-acidic MV^{2+} intercalates between the two fullerenes in triad **1** ($EC_{50} = 0.63 \pm 0.05$ mM, Figure 2c, Figure S6), thus attracting electron density from the active site (increasing intrinsic π acidity) and expanding the extent of electronic communication, including polarizability (increasing induced π acidity). In contrast to the π-acidic activator **21**, the presence of 2,7-dimethoxynaphthalene **22**[18] decreased the activity of triad **1** but not control **6** by $A/D_{(1+22)}/A/D_{(1)} = 0.79$ (Figure 3c). This inactivation was consistent with the complementary increase in electron density at the active site on the central fullerene caused by intercalation of the π base between the two fullerenes. Competitive inactivation at the active site was less likely considering the insensitivity of control **6** to **22**.

We thus conclude that remote control of anion–π catalysis on fullerene–fullerene–amine triads provides not only the most active anion–π catalyst known so far but also unprecedented direct experimental evidence that the dynamic contributions from polarizability outweigh static contributions to anion–π interactions by far. In other words, induced π acidity from the interaction of anions and anionic transition states with the giant oriented macrodipole that is generated only by their presence in polarizable π systems affords anion–π interactions with highest functional relevance. This lesson learned from fullerene-centered catalytic triads calls for a shift of paradigm from small, often fragile π surfaces with LUMOs as low, π holes as deep and quadrupoles as positive as possible to π surfaces as large and π stacks as thick and as long as possible.[19]

Acknowledgements

We thank the NMR and the MS platforms for services, and the University of Geneva, the Swiss National Centre of Competence in Research (NCCR) Molecular Systems Engineering, the NCCR Chemical Biology and the Swiss NSF for financial support. J.L.A. acknowledges a Curie fellowship (project 740288). A.B. and A.F. thank MINECO of SPAIN for financial support (projects CTQ2014-57393-C2-1-P and CTQ2017-85821-R, FEDER funds).

Conflict of interest

The authors declare no conflict of interest.

Keywords: anion–π catalysis · fullerenes · induced π acidity · polarizability

How to cite: *Angew. Chem. Int. Ed.* **2018**, *57*, 10883–10887
Angew. Chem. **2018**, *130*, 11049–11053

[1] a) M. Giese, M. Albrecht, K. Rissanen, *Chem. Commun.* **2016**, *52*, 1778–1795; b) H. T. Chifotides, K. R. Dunbar, *Acc. Chem. Res.* **2013**, *46*, 894–906; c) D.-X. Wang, M.-X. Wang, *Chimia* **2011**, *65*, 939–943; d) P. Ballester, *Acc. Chem. Res.* **2013**, *46*, 874–884; e) A. Bauzá, T. J. Mooibroek, A. Frontera, *ChemPhysChem* **2015**, *16*, 2496–2517; f) S. T. Schneebeli, M. Frasconi, Z. Liu, Y. Wu, D. M. Gardner, N. L. Strutt, C. Cheng, R. Carmieli, M. R. Wasielewski, J. F. Stoddart, *Angew. Chem. Int. Ed.* **2013**, *52*, 13100–13104; *Angew. Chem.* **2013**, *125*, 13338–13342; g) Z. Yu, A. Erbas, F. Tantakitti, L. C. Palmer, J. A. Jackman, M. Olvera de la Cruz, M.-J. Cho, S. I. Stupp, *J. Am. Chem. Soc.* **2017**, *139*, 7823–7830; h) G. Bélanger-Chabot, A. Ali, F. P. Gabbaï, *Angew. Chem. Int. Ed.* **2017**, *56*, 9958–9961; *Angew. Chem.* **2017**, *129*, 10090–10093; i) Q. He, Y. Ao, Z.-T. Huang, D.-X. Wang, *Angew. Chem. Int. Ed.* **2015**, *54*, 11785–11790; *Angew. Chem.* **2015**, *127*, 11951–11956; j) R.-B. Xu, Q.-Q. Wang, Y.-F. Ao, Z.-Y. Li, Z.-T. Huang, D.-X. Wang, *Org. Lett.* **2017**, *19*, 738–741.

[2] a) C. R. Kennedy, S. Lin, E. N. Jacobsen, *Angew. Chem. Int. Ed.* **2016**, *55*, 12596–12624; *Angew. Chem.* **2016**, *128*, 12784–12814; b) D. A. Stauffer, R. E. Barrans, Jr., D. A. Dougherty, *Angew. Chem. Int. Ed. Engl.* **1990**, *29*, 915–918; *Angew. Chem.* **1990**, *102*, 953–956; c) T. Bräuer, Q. Zhang, K. Tiefenbacher, *J. Am. Chem. Soc.* **2017**, *139*, 17500–17507; d) C. Zhao, F. D. Toste, K. N. Raymond, R. G. Bergman, *J. Am. Chem. Soc.* **2014**, *136*, 14409–14412.

[3] a) Y. Zhao, S. Benz, N. Sakai, S. Matile, *Chem. Sci.* **2015**, *6*, 6219–6223; b) Y. Cotelle, V. Lebrun, N. Sakai, T. R. Ward, S. Matile, *ACS Cent. Sci.* **2016**, *2*, 388–393.

[4] M. Akamatsu, N. Sakai, S. Matile, *J. Am. Chem. Soc.* **2017**, *139*, 6558–6561.

[5] A.-B. Bornhof, A. Bauzá, A. Aster, M. Pupier, A. Frontera, E. Vauthey, N. Sakai, S. Matile, *J. Am. Chem. Soc.* **2018**, *140*, 4884–4892.

[6] a) C. Foroutan-Nejad, Z. Badri, R. Marek, *Phys. Chem. Chem. Phys.* **2015**, *17*, 30670–30679; b) A. Frontera, D. Quinonero, C. Garau, A. Costa, P. Ballester, P. M. Deya, *J. Phys. Chem. A* **2006**, *110*, 9307–9309.

[7] a) J. López-Andarias, A. Frontera, S. Matile, *J. Am. Chem. Soc.* **2017**, *139*, 13296–13299; b) X. Zhang, L. Liu, J. López-Andarias, C. Wang, N. Sakai, S. Matile, *Helv. Chim. Acta* **2018**, *101*, e1700288.

[8] a) E. Nakamura, H. Isobe, *Acc. Chem. Res.* **2003**, *36*, 807–815; b) O. Vostrowsky, A. Hirsch, *Chem. Rev.* **2006**, *106*, 5191–5207; c) T. Da Ros, M. Prato, *Chem. Commun.* **1999**, 663–669; d) E. E. Maroto, M. Izquierdo, S. Reboredo, J. Marco-Martínez, S. Filippone, N. Martín, *Acc. Chem. Res.* **2014**, *47*, 2660–2670; e) S. Kirner, M. Sekita, D. M. Guldi, *Adv. Mater.* **2014**, *26*, 1482–1493; f) D. Bonifazi, O. Enger, F. Diederich, *Chem. Soc. Rev.* **2007**, *36*, 390–414; g) I. Nierengarten, J.-F. Nierengarten, *Chem. Asian J.* **2014**, *9*, 1436–1444; h) G. Yu, J. Gao, J. C. Hummelen, F. Wudl, A. J. Heeger, *Science* **1995**, *270*, 1789–1791.

[9] a) C.-Z. Li, C.-C. Chueh, H.-L. Yip, F. Ding, X. Li, A. K.-Y. Jen, *Adv. Mater.* **2013**, *25*, 2457–2461; b) X. Sun, W. Chen, L. Liang, W. Hu, H. Wang, Z. Pang, Y. Ye, X. Hu, Q. Wang, X. Kong, Y. Jin, M. Lei, *Chem. Mater.* **2016**, *28*, 8726–8731.

[10] a) Y. Sun, C. Cao, P. Huang, S. Yang, W. Song, *RSC Adv.* **2015**, *5*, 86082–86087; b) Y.-B. Sun, C.-Y. Cao, S.-L. Yang, P.-P. Huang, C.-R. Wang, W.-G. Song, *Chem. Commun.* **2014**, *50*, 10307–10310; c) M. Toganoh, Y. Matsuo, E. Nakamura, *J. Organomet. Chem.* **2003**, *683*, 295–300; d) S. Vidal, J. Marco-Martínez, S.

Filippone, N. Martín, *Chem. Commun.* **2017**, *53*, 4842 – 4844; e) H. Tokuyama, E. Nakamura, *J. Org. Chem.* **1994**, *59*, 1135 – 1138.
[11] D. S. Sabirov, *RSC Adv.* **2014**, *4*, 44996 – 45028.
[12] a) T. E. Shubina, D. I. Sharapa, C. Schubert, D. Zahn, M. Halik, P. A. Keller, S. G. Pyne, S. Jennepalli, D. M. Guldi, T. Clark, *J. Am. Chem. Soc.* **2014**, *136*, 10890 – 10893; b) F. J. Rizzuto, D. M. Wood, T. K. Ronson, J. R. Nitschke, *J. Am. Chem. Soc.* **2017**, *139*, 11008 – 11011.
[13] a) M. E. El-Khouly, J. H. Kim, K.-Y. Kay, C. S. Choi, O. Ito, S. Fukuzumi, *Chem. Eur. J.* **2009**, *15*, 5301 – 5310; b) M. Supur, M. E. El-Khouly, J. H. Seok, K.-Y. Kay, S. Fukuzumi, *J. Phys. Chem. A* **2011**, *115*, 14430 – 14437.
[14] a) M. Rudolf, O. Trukhina, J. Perles, L. Feng, T. Akasaka, T. Torres, D. M. Guldi, *Chem. Sci.* **2015**, *6*, 4141 – 4147; b) O. Trukhina, M. Rudolf, G. Bottari, T. Akasaka, L. Echegoyen, T. Torres, D. M. Guldi, *J. Am. Chem. Soc.* **2015**, *137*, 12914 – 12922; c) L. Feng, M. Rudolf, S. Wolfrum, A. Troeger, Z. Slanina, T. Akasaka, S. Nagase, N. Martín, T. Ameri, C. J. Brabec, D. M. Guldi, *J. Am. Chem. Soc.* **2012**, *134*, 12190 – 12197.
[15] F. N. Miros, S. Matile, *ChemistryOpen* **2016**, *5*, 219 – 226.
[16] a) X. Tan, D. I. Schuster, S. R. Wilson, *Tetrahedron Lett.* **1998**, *39*, 4187 – 4190; b) S. Filippone, E. E. Maroto, Á. Martín-Domenech, M. Suarez, N. Martín, *Nat. Chem.* **2009**, *1*, 578 – 582; c) E. E. Maroto, S. Filippone, Á. Martín-Domenech, M. Suarez, N. Martín, *J. Am. Chem. Soc.* **2012**, *134*, 12936 – 12938.
[17] a) J. Iehl, M. Frasconi, H.-P. Jacquot de Rouville, N. Renaud, S. M. Dyar, N. L. Strutt, R. Carmieli, M. R. Wasielewski, M. A. Ratner, J.-F. Nierengarten, J. F. Stoddart, *Chem. Sci.* **2013**, *4*, 1462 – 1469; b) G. Casella, G. Saielli, *New J. Chem.* **2011**, *35*, 1453 – 1459.
[18] S. Hagihara, H. Tanaka, S. Matile, *J. Am. Chem. Soc.* **2008**, *130*, 5656 – 5657.
[19] Molecular models of homologous fullerene–fullerene–fullerene–amine tetrads gave a polarizability of $\alpha = 2240$ a.u., that is $+741$ a.u. compared to triad **1** and $+1337$ a.u. compared to dyad **6**. Synthesis of these tetrads has failed so far due to solubility problems.

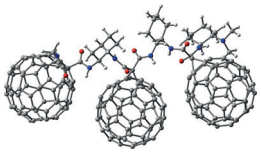

Manuscript received: April 6, 2018
Version of record online: May 22, 2018

